arXiv:2106.14914v1 [cond-mat.mes-hall] 28 Jun 2021

Non-Hermitian Higher-Order Dirac Semimetals

Sayed Ali Akbar Ghorashi,[1,*] Tianhe Li,[2] Masatoshi Sato,[3] and Taylor L. Hughes[2]

[1] *Department of Physics, William & Mary, Williamsburg, Virginia 23187, USA*
[2] *Department of Physics and Institute for Condensed Matter Theory, University of Illinois at Urbana-Champaign, IL 61801, USA*
[3] *Yukawa Institute for Theoretical Physics, Kyoto University, Kyoto 606-8502, Japan*

(Dated: August 21, 2021)

In this article we study 3D non-Hermitian higher-order Dirac semimetals (NHHODSMs). Our focus is on C_4-symmetric non-Hermitian systems where we investigate inversion ($\mathcal{I}$) or time-reversal ($\mathcal{T}$) symmetric models of NHHODSMs having real bulk spectra. We show that they exhibit the striking property that the bulk and surfaces are anti-PT and PT symmetric, respectively, and so belong to two different topological classes realizing a novel non-Hermitian topological phase which we call a *hybrid-PT topological phases*. Interestingly, while the bulk spectrum is still fully real, we find that exceptional Fermi-rings (EFRs) appear connecting the two Dirac nodes on the surface. This provides a route to probe and utilize both the bulk Dirac physics and exceptional rings/points on equal footing. Moreover, particularly for $\mathcal{T}$-NHHODSMs, we also find real hinge-arcs connecting the surface EFRs. We show that this higher-order topology can be characterized using a biorthogonal real-space formula of the quadrupole moment. Furthermore, by applying Hermitian C_4-symmetric perturbations, we discover various novel phases, particularly: (i) an intrinsic $\mathcal{I}$-NHHODSM having hinge arcs and gapped surfaces, and (ii) a novel $\mathcal{T}$-symmetric skin-topological HODSM which possesses both topological and skin hinge modes. The interplay between non-Hermition and higher-order topology in this work paves the way toward uncovering rich phenomena and hybrid functionality that can be readily realized in experiment.

Introduction.– Topological phases matter have been on the frontier of condensed matter and related areas of research over last two decades [1, 2]. Recently, two new research directions have garnered attention: higher-order topology and non-Hermitian topological phases. The hallmark of a d-dimensional nth-order topological phase is a gapped bulk harboring robust boundary states/features with co-dimension $p = d - n$[3–14]. Higher order topological systems have been experimentally observed in various physical platforms [15–20]. Along with this, non-Hermitian topological phases are inherently realized in non-equilibrium contexts, and show many interesting properties with broad applications ranging from photonics to ultracold atoms[21–25]. Similar to Hermitian topological phases, the topological classification of non-Hermitian phases has been extensively explored [26–30]. Interestingly, the notion of bulk-boundary correspondence for non-Hermitian systems has proven to be subtle, primarily due to the emergence of exceptional structures (ESs) (points/rings/disks), on which eigenstates and eigenenergies coalesce in complex energy space [21, 22, 31], as well as the phenomenon of the non-Hermitian skin effect where there is an extensive localization of states on the boundaries[21, 32–43].

In this work, we study the interplay of higher- order and non-Hermitian topological phases in the context of higher order topological semimetals. While previous studies have mostly explored two-dimensional and/or gapped phases [44–48], the three-dimensional non-Hermitian semimetallic phases remain unexplored. We will begin by introducing non-Hermitian perturbations to a previously studied C_4^z-symmetric higher-order Dirac semimetal (HODSMs) [49]. From this we will identify two novel phases: an $\mathcal{I}$-symmetric and a $\mathcal{T}$-symmetric non-Hermitian Dirac semimetal (NHDSM). These phases feature real bulk spectra having point Dirac

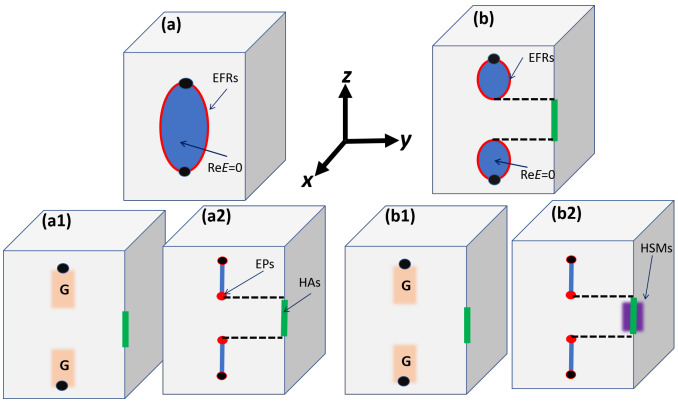


FIG. 1. The schematic summary of results. (a) $\mathcal{I}$-symmetric NHHODSMs can possess surface exceptional Fermi-rings (EFRs) connecting the projection of the real bulk Dirac nodes (black dots) on the surface and no hinge arcs (HAs) while (b) $\mathcal{T}$-symmetric NHHODSMs can exhibit two patches of surface EFRs connected by HAs (green line on the hinge). (a1, b1) have turned on the α_1 perturbation (a1,b1) for both models. In both cases the EFRs gap out and HAs appear. (a2,b2) have α_2 turned on for both models. This perturbation deforms the EFRs to exceptional points (EPs), [note that the projection of the real bulk Dirac nodes and two of EPs coincide] to form two exceptional Fermi-arcs on the surface which are connected by HAs on the hinges. (b2) Also possess hinge skin modes (HSMs) [shaded purple region] coexisting with HAs.

nodes, and a variety of complex surface spectra. Strikingly, the bulk and surface in these phases possess anti-PT and PT symmetry respectively, and hence belong to two different classes of the non-Hermitian topological classification. This allows for new types of *hybrid-PT non-Hermitian topological phases* where the bulk and surface ESs are protected by different symmetries. Both the $\mathcal{I}$ and $\mathcal{T}$-symmetric NHDSMs we study host exceptional Fermi ring (EFR) surface modes protected by symmetries of the non-Hermtian $\mathcal{P}$CI class. Additionally, the $\mathcal{T}$-symmetric phase hosts real hinge arcs (HAs), which can be characterized by a quantized bulk, biorthogonal quadrupole moment, and represents an unprecedented non-Hermitian higher order Dirac semimetal (NHHODSM) phase. Furthermore, by breaking the symmetries that protect the surface EFRs while preserving the bulk C_4^z symmetry, we unveil various novel phases including: (i) an $\mathcal{I}$-NHHODSM having exceptional Fermi-arcs on the surface coexisting with intrinsic hinge arcs having complex energies, (ii) a $\mathcal{T}$-symmetric skin-topological NHHODSM which shows both the hinge skin modes (HSMs) and complex HAs.

Models.—To illustrate all of the phenomena mentioned above we can start with a parent Hermitian model of a HODSM introduced in [49],

$$H_{HODSM}(\mathbf{k}) = \sum_{i=1}^{4} a_i(\mathbf{k})\Gamma_i, \tag{1}$$

where $a_1(\mathbf{k}) = \sin(k_y)$, $a_2(\mathbf{k}) = \left(\gamma + \frac{1}{2}\cos k_z + \cos k_y\right)$, $a_3(\mathbf{k}) = \sin(k_x)$, $a_4(\mathbf{k}) = \left(\gamma + \frac{1}{2}\cos k_z + \cos k_x\right)$, and the $\{\Gamma_\alpha\}$ are direct products of Pauli matrices, σ_i, κ_i: $\Gamma_0 = \sigma^3\kappa^0, \Gamma_i = -\sigma^2\kappa^i$ for $i = 1,2,3$, and $\Gamma_4 = \sigma^1\kappa^0$. The parameter γ represents the intra-cell coupling, and we have set the amplitudes of the inter-cell couplings to 1. This model preserves C_4^z, mirror $\mathcal{M}_{x,y,z}$, inversion, $\mathcal{I}$, and time-reversal $\mathcal{T} = K$ [50] symmetries. We focus on the parameter regime $-0.5 < \gamma < -1.5$ where Eq. (1) generates a higher order Dirac semimetal spectrum exhibiting two gapless Dirac nodes in the bulk, gapped surfaces, and Fermi arcs connecting the nodes at the hinges. From this parent state we will investigate both inversion and time-reversal symmetric non-Hermitian perturbations and discuss some resulting topological phases.

$\mathcal{I}$-Model.— First we will consider the following non-Hermitian $\mathcal{I}$ symmetric model,

$$H_D^{\mathcal{I}} = H_{HODSM}(\mathbf{k}) + im_1\Gamma_0 a_0(\mathbf{k}), \tag{2}$$

where $a_0(\mathbf{k}) = (\cos(k_x) - \cos(k_y))$, and m_1 is a real constant. The m_1 term breaks $\mathcal{M}_{x,y}$ symmetries while keeping $\mathcal{I}$ and C_4^z. Interestingly, while $m_1 \neq 0$ breaks $\mathcal{T}$ and hence $\mathcal{IT}$, it preserves the anti-PT symmetry $(\mathcal{IT})H(\mathbf{k})(\mathcal{IT})^\dagger = -H(\mathbf{k})$. Moreover, reciprocity $\mathcal{R}H(\mathbf{k})\mathcal{R}^\dagger = H^T(-\mathbf{k})$ and $\mathcal{IR}$ are also preserved, where

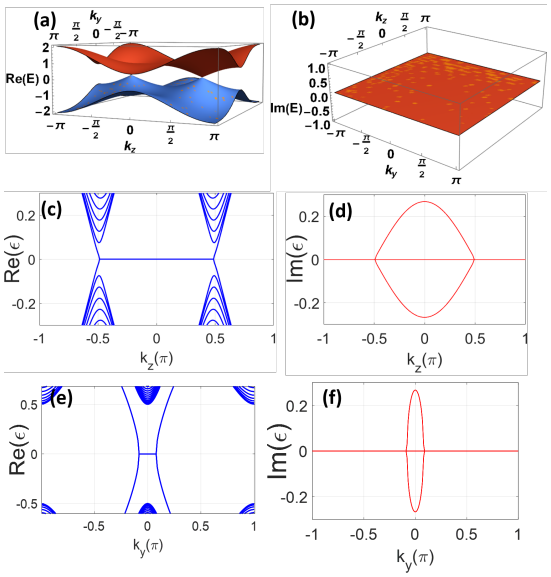


FIG. 2. The spectrum of $H^{\mathcal{I}}$ with $\gamma = -1$, $m_1 = -0.75\,(< m_1^c)$. (a,b) The real and imaginary parts of the bulk spectrum in the $k_y - k_z$-plane with periodic boundary conditions in all directions, (c,d) the real and imaginary spectrum for open boundaries conditions in the x-direction which depicts EFRs along the $k_z - axis$, $(k_y = 0)$, (e,f) are similar to (c,d) except plotted along the $k_y - axis$, $(k_z = 0)$.

$\mathcal{R} = \mathbb{I}$. These symmetries, along with the chiral symmetry $\Gamma_0 H(\mathbf{k})\Gamma_0^\dagger = -H^\dagger(\mathbf{k})$, place Eq. (2) in the class $\mathcal{P}$CII† [29]. Remarkably, the bulk spectrum remains fully real up to a critical value of m_1^c. To see this we calculate the eigenvalues of Eq. (2): $E(\mathbf{k}) = \pm\sqrt{\sum_i^4 a_i^2(\mathbf{k}) - m_1^2 a_0^2(\mathbf{k})}$. The spectrum becomes complex at a given $\mathbf{k_0}$ only when $m_1 > m_1^c \equiv \min_{\mathbf{k_0}} \sum_i^4 a_i^2(\mathbf{k}_0)/a_0^2(\mathbf{k}_0)$ (if $a_0^2(\mathbf{k}_0) = 0$ this never happens). When the bulk energies become complex, 3D ESs form that project to four-fold degenerate exceptional rings in the $k_y - k_z$ and $k_x - k_z$ planes centered around $(k_x, k_z) = (\pi, 0)$ and $(k_y, k_z) = (\pi, 0)$, respectively (see [51]). Unlike many previous cases [21] the ESs here emerge from the bulk away from the locations of the real Dirac nodes and not by transforming the gapless Dirac points to exceptional rings (or pair of EPs). Therefore, in this system the real Dirac nodes and the bulk ESs can coexist. For the remainder of this article we focus on the regime of $m_1 < m_1^c$ where the bulk spectrum is fully real. Remarkably, for some $m_1 < m_1^c$, the real HAs are destroyed and the surface develops EFRs formed between the projection of the two Dirac nodes (Fig. 2). Unlike previous work[27, 52, 53], the surface EFRs do not emanate from an existing real state, since the surface in the Hermitian limit, $m_1 = 0$, is gapped. Instead, they suddenly appear in the gapped region between projections of the two bulk Dirac nodes simultaneously with the gapping out of the HAs. As mentioned above, when further increasing m_1 to

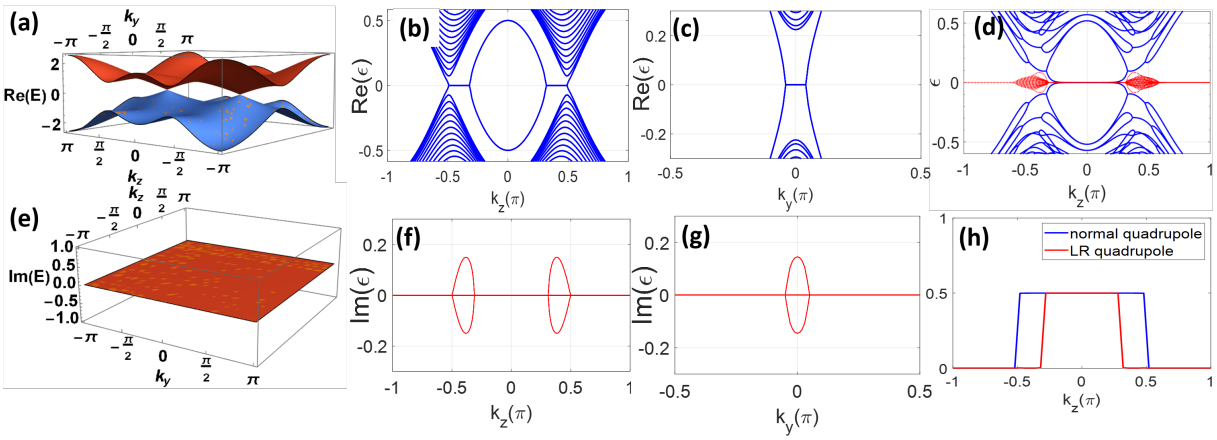


FIG. 3. The spectrum of $\mathcal{T}$-NHHODSM with $\gamma = -1$, $m = -0.85$. The real and imaginary parts of the bulk spectrum in the $k_y - k_z$-plane are shown in (a,e). Real and imaginary spectra for open boundaries in x are shown for (b,f) the k_z-axis, (c,g) the line (k_y, $k_z = 0.45\pi$). (d) the real (blue) and imaginary (red) spectra for open boundaries in x and y along k_z. (h) The q_{xy}^{RR} (blue) and q_{xy}^{LR} vs. k_z.

$m_1 > m_1^c$, the bulk spectrum becomes complex and the projections of the bulk ESs on the surfaces are shown in [51].

Now let us discuss the topological protection of the surface EFRs in Fig. 2(c-f). On the x-surface, the $H_D^{\mathcal{I}}$ in (2) hosts $\mathcal{R}$, $\mathcal{TM}_y$, $\mathcal{M}_z$, Γ_0 symmetries. However, only the product $\mathcal{TM}_y\mathcal{M}_z$ and Γ_0 keep the surface momentum (k_y, k_z) invariant, and thus may protect non-Hermitian gapless structures at an arbitrary position in momentum space. Since $(\mathcal{TM}_y\mathcal{M}_z)^2 = 1$ and $\{\mathcal{TM}_y\mathcal{M}_z, \Gamma\} = 0$, these symmetries define class $\mathcal{P}$CI[29]. The surface possesses a point gap, and since the surface EFRs shown in Fig. 2(c-f)[also Fig. 1(a)] are co-dimension 1 exceptional rings, the EFRs can be characterized by a $\mathbb{Z}$ topological invariant[54] which protects the degeneracies. We note that the bulk and surface having ESs protected by different symmetries is remarkable because it again shows the complicated bulk-boundary correspondence for non-Hermitian systems. More strikingly, since the bulk and surface are anti-PT and PT symmetric, respectively, both PT and anti-PT applications can be exploited in a single system in a natural way[55]. We call this new family of non-Hermitian topological phases, the *hybrid-PT topological phases*.

$\mathcal{T}$-Model.—Next we will consider perturbing Eq. 1 with a non-Hermtian term that preserves $\mathcal{T}$:

$$H_D^{\mathcal{T}} = H_{HODSM}(\mathbf{k}) + im_2\Gamma_0 a_0(\mathbf{k})\sin(k_z). \qquad (3)$$

Similar to $H_D^{\mathcal{I}}$, Eq. (3) belongs to class $\mathcal{P}$CII† and possesses anti-PT symmetry. As before, the bulk spectrum of (3) becomes complex only when $m_2 > m_2^c = \min_{\mathbf{k_0}} \sum_i^4 a_i^2(\mathbf{k}_0)/(a_0(\mathbf{k}_0)\sin(k_{z0}))^2$ [56]. Similar to the case of $H^{\mathcal{I}}$, as m_2 is increased from zero, the surface spectrum (on surfaces normal to $\hat{x}$ or $\hat{y}$) becomes complex before the bulk. However, in this regime, unlike the $\mathcal{I}$-symmetric model, here the two Dirac nodes are connected by two EFRs which are separated by a real gap in the middle of the spectrum (Fig. 3(b)). Remarkably, by further opening boundary along the x and y-directions to get a hinge, we find Fermi hinge-arcs that survive in a region corresponding to the gapped region of the surface states (Fig. 3(d)). Interestingly, the hinge arcs connected the two EFRs on the surface instead of bulk Dirac nodes. Thus, the model in (3), is a type of NHHODSM which we call *hybrid-order exceptional Dirac semimetal* since it has surface EFRs and hinge states. As for symmetries, the surface EFRs on a surface perpendicular to the x-direction, $\mathcal{TM}_y\mathcal{M}_z$ and Γ_0 symmetries are preserved. Thus, we obtain the same topological classification class $\mathcal{P}$CI for the surface EFRs like the $\mathcal{I}$-symmetric case. Therefore, we find that the $H_D^{\mathcal{T}}$ like $H_D^{\mathcal{I}}$ is a hybrid-order PT topological phase exhibit anti-PT and PT symmetries in the bulk and surfaces, respectively.

Topological invariant.— To characterize the higher-order topology in the presence of non-Hermitian perturbations, we will adapt the calculation of the quadrupole moment q_{xy} a non-Hermitian context. To do so, we employ the real-space, operator-based, formula [57–59]. This bulk characteristic is crucial because of the complications due to the non-Hermitian bulk-boundary correspondence, e.g., explicitly calculating the corner charge and surface polarization (and hence q_{xy}) in non-Hermitian systems may be challenging due to ESs or the skin-effect. Let us now show that this formalism correctly captures the existence of zero-energy modes on the hinges in both the $\mathcal{I}$ and $\mathcal{T}$-symmetric models, provided we use

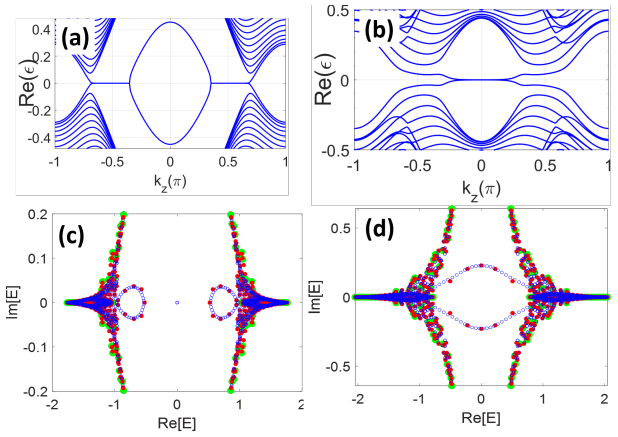


FIG. 4. The real part of the spectrum of for Eq. (2) having $\gamma = -0.7$, $m_1 = 0.75$, $\alpha_2 = 0.1$ along (a) the k_z-axis for open-boundaries in the x-direction and (b) similar to (a) but with open boundaries along x and y to show hinge states. Next we show the complex-spectrum for $H_D^{\mathcal{T}}$ with the $\alpha_2 = 0.1$, for (c) $k_z = 0.25\pi$ (i.e., hinge states present) and (d) $k_z = 0.4\pi$ (i.e., hinge states absent). The filled green and red dots denote full periodic boundary conditions and x-open/y-periodic, respectively, while blue circles show the case when both x, y are open boundaries. $L_x = 20$, $L_y = 20$ for all the boundary conditions in (c,d).

a biorthogonal basis [32]:

$$q_{xy} = \frac{1}{2\pi}\,\mathrm{Im}\left[\ln\langle\Psi^{R(L)}|\hat{U}_{xy}|\Psi^{R(L)}\rangle\right] \tag{4}$$

where $\hat{U}_{xy} = e^{2\pi i\sum_r r_x r_y \hat{n}_r/(L_x L_y)}$, $|\Psi^{R(L)}\rangle = \prod_{n\in occ}\gamma^\dagger_{n,R(L)}|0\rangle$, $\Psi^{R(L)}$ denote the right and left eigenvectors, and r_x (L_x) and r_y (L_y) are the coordinates (sample size) along the x and y directions, respectively. Figure 3(h), shows the q_{xy} for the model in Eq. (3) calculated using both normal (RR) and biorthogonal, LR, approaches. Interestingly, the LR approach returns the correct value, i.e, it depicts quantized $q_{xy} = 0.5$ for the region of momentum space in which there exist gapless hinge arcs, in the regime when the surface has EFRs, but the bulk is still fully real. Additionally, for $H_D^{\mathcal{I}}$, we find the $q_{xy}^{LR} = 0$ for all k_z. In comparison, for both $H_D^{\mathcal{T}}$ and $H_D^{\mathcal{I}}$ q_{xy}^{RR} returns 0.5 for any k_z between the bulk Dirac nodes, even for k_z where there are no hinge-arcs such as the $H_D^{\mathcal{I}}$ case [51].

Alternative Surface Phenomena.— By breaking some of the protective non-Hermitian symmetries of the surface we can generate other types of hybrid surface/hinge phenomena. To show this, let us investigate the effect of Hermitian perturbations which leave the bulk Dirac nodes intact, and preserve the bulk C_4^z symmetry, while breaking the surface protective non-Hermitian symmetries. The first example is $\alpha_1\Gamma_0 a_0(\mathbf{k})$ ($\alpha_1\Gamma_0 a_0(\mathbf{k})\sin(k_z)$), with strength α_1 for the $H_D^{\mathcal{I}}$ ($H_D^{\mathcal{T}}$) model. In the case of $H_D^{\mathcal{I}}$ any bulk ESs (i.e., if $m_1 > m_1^c$) become gapped when $\alpha_1 \neq 0$, while the real Dirac nodes remain gapless. The surface EFRs become gapped as well, however, since the perturbation gaps out the x and y surfaces with opposite signs, a non-zero α_1 induces hinge domain walls (Fig. 1(a1)). Interestingly, the resulting phase is a $2nd$-order $\mathcal{I}$-NHHODSM having two Dirac nodes in the bulk and hinge states despite having no hinge modes when $\alpha_1 = 0$. Next, for $H_D^{\mathcal{T}}$ with $\alpha_1 \neq 0$, the bulk Dirac nodes remain gapless, and any bulk ESs are gapped. Moreover, the surface EFRs also become gapped while the hinge states remain intact (Fig. 1(b1)). Interestingly, even though the surface EFRs are gapped, the hinges remain arc-like and their lengths remain same as the case of $\alpha_1 = 0$ and so the systems is still a $\mathcal{T}$-NHHODSM.

To illustrate a second set of behaviors we consider adding the term $\alpha_2\sigma^3\kappa^2 a_0(\mathbf{k})(\alpha_2\sigma^3\kappa^2 a_0(\mathbf{k})\sin(k_z))$ for $H_D^{\mathcal{I}}$ ($H_D^{\mathcal{T}}$). Like the previous case, $\alpha_2 \neq 0$ gaps out the bulk ESs for both $H_D^{\mathcal{I}}$, and $H_D^{\mathcal{T}}$ while preserving the real, bulk Dirac nodes. However, these terms do not fully gap out the surface EFRs, but instead deform them to EPs forming what we call an *exceptional Fermi-arc*, i.e, a surface Fermi-arc terminated by an EPs instead of a conventional nodal point (Fig. 1(a2,b2)). Additionally, for the case of open boundary conditions in both the x and y-directions we find the following remarkable results: (i) considering $H_D^{\mathcal{I}}$ having $\alpha_2 \neq 0$, we find that in the middle of the exceptional surface Fermi-arcs a gap opens up, as γ is tuned, and hinge-arcs appear in the surface gap (Fig. 4(b)) characterized by a quantized q_{xy}^{LR} (see [51]). We recall that $H_D^{\mathcal{I}}$ with $\alpha_2 = 0$ does not possess hinge-arcs, therefore, $H_D^{\mathcal{I}}$ with non-zero α_2 becomes an *intrinsic hybrid-order non-Hermitian Dirac semimetal*. (ii) Considering $H_D^{\mathcal{T}}$ and non-zero α_2, we find that the HAs remain intact (having $q_{xy}^{LR} = 0.5$) since α_2 preserves C_4^z. Interestingly, the surface spectra, in the same region of k_z-space that the real HAs exist, develops complex loop spectra. For example, Figure. 4(c,d) shows the complex spectra under various boundary conditions for a fixed-k_z slice in the region of momentum space with and without HAs. Interestingly, for each value of k_z in the region exhibiting HAs we find the formation of two loops having a point-gap with non-vanishing winding in the complex energy spectra (see Fig. 4(c)), which disappear as k_z is tuned and the two loops close/merge along imaginary axis (see Fig. 4(d)). The result is that for each value of k_z for which the real HAs exist there are also $\mathcal{O}(L)$ corner skin modes that appear which arise from the complex surface states[60–62]. Therefore, we find a novel $3d$ non-Hermitian topological semimetal having coexisting real HAs and hinge skin modes (HSMs), which we call a *higher-order skin-topological Dirac semimetal*.

Concluding remarks.—We have investigated higher-order Dirac semimetals in the presence of C_4^z-symmetric non-Hermitian perturbations. We have shown that they exhibit the striking property that bulk and surfaces are

anti-PT and PT symmetric, respectively, realizing a novel non-Hermitian topological phase which we dubbed, a hybrid-PT topological phase. These systems may open up new avenues for many fundamental and practical directions, such as novel topological lasers, sensors and photonics [55, 63–66] with selected utilization of anti-PT/PT on the bulk/surface. In our models in the bulk, real Dirac nodes and ESs coexist, providing a platform for utilizing both Dirac and exceptional physics in the bulk as well as surfaces in the same system. Moreover, we revealed that they show a unique edge-gain (complex surface) without bulk-gain (real bulk).

Finally we make brief remarks on plausible experimental directions. The main building block of models discussed here, i.e., stacks of 2D quadrupole insulators have been realized in variety of platforms both in Hermitian [15–20] and non-Hermitian [47] systems. Recently, 3D models of Hermitian HOSMs have been implemented in experiments [67–70]. Therefore, the physics discussed in this work is readily accessible and can motivate an immediate experimental realization of NHHODSMs.

Acknowledgement.—S.A.A.G acknowledges support from ARO (Grant No. W911NF-18-1-0290) and NSF (Grant No. DMR1455233). T.L. and T.L.H. thank the US Office of Naval Research (ONR) Multidisciplinary University Research Initiative (MURI) grant N00014-20-1-2325 on Robust Photonic Materials. M.S. was supported by JST CREST Grant No. JPMJCR19T2, Japan, and KAKENHI Grant No. JP20H00131 from the JSPS.

* sghorashi@wm.edu

[1] Ching-Kai Chiu, Jeffrey C. Y. Teo, Andreas P Schnyder, and Shinsei Ryu, "Classification of topological quantum matter with symmetries," Reviews of Modern Physics **88**, 035005 (2016).

[2] N. P. Armitage, E. J. Mele, and Ashvin Vishwanath, "Weyl and dirac semimetals in three-dimensional solids," Rev. Mod. Phys. **90**, 015001 (2018).

[3] Wladimir A Benalcazar, B Andrei Bernevig, and Taylor L Hughes, "Quantized electric multipole insulators." Science **357**, 61–66 (2017).

[4] Wladimir A Benalcazar, B Andrei Bernevig, and Taylor L Hughes, "Selected for a Viewpoint in Physics Electric multipole moments, topological multipole moment pumping, and chiral hinge states in crystalline insulators," Physical Review B **96**, 245115 (2017).

[5] Frank Schindler, Ashley M. Cook, Maia G. Vergniory, Zhijun Wang, Stuart S. P. Parkin, B. Andrei Bernevig, and Titus Neupert, "Higher-order topological insulators," Science Advances **4**, eaat0346 (2018).

[6] Frank Schindler, Zhijun Wang, Maia G. Vergniory, Ashley M. Cook, Anil Murani, Shamashis Sengupta, Alik Yu. Kasumov, Richard Deblock, Sangjun Jeon, Ilya Drozdov, Hélène Bouchiat, Sophie Guéron, Ali Yazdani, B. Andrei Bernevig, and Titus Neupert, "Higher-order topology in bismuth," Nature Physics **14**, 918–924 (2018).

[7] Zhida Song, Zhong Fang, and Chen Fang, "$(d-2)$-dimensional edge states of rotation symmetry protected topological states," Phys. Rev. Lett. **119**, 246402 (2017).

[8] Josias Langbehn, Yang Peng, Luka Trifunovic, Felix von Oppen, and Piet W. Brouwer, "Reflection-symmetric second-order topological insulators and superconductors," Phys. Rev. Lett. **119**, 246401 (2017).

[9] Wladimir A. Benalcazar, Tianhe Li, and Taylor L. Hughes, "Quantization of fractional corner charge in C_n-symmetric higher-order topological crystalline insulators," Phys. Rev. B **99**, 245151 (2019).

[10] Tianhe Li, Penghao Zhu, Wladimir A. Benalcazar, and Taylor L. Hughes, "Fractional disclination charge in two-dimensional C_n-symmetric topological crystalline insulators," Phys. Rev. B **101**, 115115 (2020).

[11] Sayed Ali Akbar Ghorashi, Xiang Hu, Taylor L. Hughes, and Enrico Rossi, "Second-order dirac superconductors and magnetic field induced majorana hinge modes," Phys. Rev. B **100**, 020509 (2019).

[12] Sayed Ali Akbar Ghorashi, Taylor L. Hughes, and Enrico Rossi, "Vortex and surface phase transitions in superconducting higher-order topological insulators," Phys. Rev. Lett. **125**, 037001 (2020).

[13] Sayed Ali Akbar Ghorashi, Tianhe Li, and Taylor L. Hughes, "Higher-order weyl semimetals," Phys. Rev. Lett. **125**, 266804 (2020).

[14] Dumitru Călugăru, Vladimir Juričić, and Bitan Roy, "Higher-order topological phases: A general principle of construction," Phys. Rev. B **99**, 041301 (2019).

[15] Christopher W. Peterson, Wladimir A. Benalcazar, Taylor L. Hughes, and Gaurav Bahl, "A quantized microwave quadrupole insulator with topologically protected corner states," Nature **555**, 346–350 (2018).

[16] Jiho Noh, Wladimir A. Benalcazar, Sheng Huang, Matthew J. Collins, Kevin P. Chen, Taylor L. Hughes, and Mikael C. Rechtsman, "Topological protection of photonic mid-gap defect modes," Nature Photonics **12**, 408–415 (2018).

[17] Marc Serra-Garcia, Valerio Peri, Roman Süsstrunk, Osama R. Bilal, Tom Larsen, Luis Guillermo Villanueva, and Sebastian D. Huber, "Observation of a phononic quadrupole topological insulator," Nature **555**, 342–345 (2018).

[18] Stefan Imhof, Christian Berger, Florian Bayer, Johannes Brehm, Laurens W. Molenkamp, Tobias Kiessling, Frank Schindler, Ching Hua Lee, Martin Greiter, Titus Neupert, and Ronny Thomale, "Topolectrical-circuit realization of topological corner modes," Nature Physics **14**, 925–929 (2018).

[19] Xiang Ni, Matthew Weiner, Andrea Alù, and Alexander B Khanikaev, "Observation of higher-order topological acoustic states protected by generalized chiral symmetry," Nature materials **18**, 113–120 (2019).

[20] Haoran Xue, Yahui Yang, Fei Gao, Yidong Chong, and Baile Zhang, "Acoustic higher-order topological insulator on a kagome lattice," Nature materials **18**, 108–112 (2019).

[21] Emil J. Bergholtz, Jan Carl Budich, and Flore K. Kunst, "Exceptional topology of non-hermitian systems," Rev. Mod. Phys. **93**, 015005 (2021).

[22] Yuto Ashida, Zongping Gong, and Masahito Ueda, "Non-hermitian physics," Advances in Physics **69**, 249–435 (2020).

[23] Hengyun Zhou, Chao Peng, Yoseob Yoon, Chia Wei

Hsu, Keith A Nelson, Liang Fu, John D Joannopoulos, Marin Soljačić, and Bo Zhen, "Observation of bulk fermi arc and polarization half charge from paired exceptional points," Science **359**, 1009–1012 (2018).
[24] Alexander Cerjan, Sheng Huang, Mohan Wang, Kevin P Chen, Yidong Chong, and Mikael C Rechtsman, "Experimental realization of a weyl exceptional ring," Nature Photonics **13**, 623–628 (2019).
[25] He Gao, Haoran Xue, Zhongming Gu, Tuo Liu, Jie Zhu, and Baile Zhang, "Non-hermitian route to higher-order topology in an acoustic crystal," Nature Communications **12** (2021), 10.1038/s41467-021-22223-y.
[26] Zongping Gong, Yuto Ashida, Kohei Kawabata, Kazuaki Takasan, Sho Higashikawa, and Masahito Ueda, "Topological phases of non-hermitian systems," Phys. Rev. X **8**, 031079 (2018).
[27] Kohei Kawabata, Ken Shiozaki, Masahito Ueda, and Masatoshi Sato, "Symmetry and topology in non-hermitian physics," Phys. Rev. X **9**, 041015 (2019).
[28] Chun-Hui Liu, Hui Jiang, and Shu Chen, "Topological classification of non-hermitian systems with reflection symmetry," Phys. Rev. B **99**, 125103 (2019).
[29] Kohei Kawabata, Takumi Bessho, and Masatoshi Sato, "Classification of exceptional points and non-hermitian topological semimetals," Phys. Rev. Lett. **123**, 066405 (2019).
[30] Hengyun Zhou and Jong Yeon Lee, "Periodic table for topological bands with non-hermitian symmetries," Phys. Rev. B **99**, 235112 (2019).
[31] WD Heiss, "The physics of exceptional points," Journal of Physics A: Mathematical and Theoretical **45**, 444016 (2012).
[32] Flore K. Kunst, Elisabet Edvardsson, Jan Carl Budich, and Emil J. Bergholtz, "Biorthogonal bulk-boundary correspondence in non-hermitian systems," Phys. Rev. Lett. **121**, 026808 (2018).
[33] Nobuyuki Okuma, Kohei Kawabata, Ken Shiozaki, and Masatoshi Sato, "Topological origin of non-hermitian skin effects," Phys. Rev. Lett. **124**, 086801 (2020).
[34] Shunyu Yao and Zhong Wang, "Edge states and topological invariants of non-hermitian systems," Phys. Rev. Lett. **121**, 086803 (2018).
[35] Fei Song, Shunyu Yao, and Zhong Wang, "Non-hermitian skin effect and chiral damping in open quantum systems," Phys. Rev. Lett. **123**, 170401 (2019).
[36] VM Martinez Alvarez, JE Barrios Vargas, Matias Berdakin, and LEF Foa Torres, "Topological states of non-hermitian systems," The European Physical Journal Special Topics **227**, 1295–1308 (2018).
[37] V. M. Martinez Alvarez, J. E. Barrios Vargas, and L. E. F. Foa Torres, "Non-hermitian robust edge states in one dimension: Anomalous localization and eigenspace condensation at exceptional points," Phys. Rev. B **97**, 121401 (2018).
[38] Lei Xiao, Tianshu Deng, Kunkun Wang, Gaoyan Zhu, Zhong Wang, Wei Yi, and Peng Xue, "Non-hermitian bulk–boundary correspondence in quantum dynamics," Nature Physics **16**, 761–766 (2020).
[39] Linhu Li, Ching Hua Lee, and Jiangbin Gong, "Topological switch for non-hermitian skin effect in cold-atom systems with loss," Phys. Rev. Lett. **124**, 250402 (2020).
[40] Deyuan Zou, Tian Chen, Wenjing He, Jiacheng Bao, Ching Hua Lee, Houjun Sun, and Xiangdong Zhang, "Observation of hybrid higher-order skin-topological effect in non-hermitian topolectrical circuits," (2021), arXiv:2104.11260 [cond-mat.mes-hall].
[41] Tobias Helbig, Tobias Hofmann, S Imhof, M Abdelghany, T Kiessling, LW Molenkamp, CH Lee, A Szameit, M Greiter, and R Thomale, "Generalized bulk–boundary correspondence in non-hermitian topolectrical circuits," Nature Physics **16**, 747–750 (2020).
[42] Ananya Ghatak, Martin Brandenbourger, Jasper van Wezel, and Corentin Coulais, "Observation of non-hermitian topology and its bulk–edge correspondence in an active mechanical metamaterial," Proceedings of the National Academy of Sciences **117**, 29561–29568 (2020).
[43] Sebastian Weidemann, Mark Kremer, Tobias Helbig, Tobias Hofmann, Alexander Stegmaier, Martin Greiter, Ronny Thomale, and Alexander Szameit, "Topological funneling of light," Science **368**, 311–314 (2020).
[44] Tao Liu, Yu-Ran Zhang, Qing Ai, Zongping Gong, Kohei Kawabata, Masahito Ueda, and Franco Nori, "Second-order topological phases in non-hermitian systems," Phys. Rev. Lett. **122**, 076801 (2019).
[45] Motohiko Ezawa, "Non-hermitian higher-order topological states in nonreciprocal and reciprocal systems with their electric-circuit realization," Phys. Rev. B **99**, 201411 (2019).
[46] Elisabet Edvardsson, Flore K. Kunst, and Emil J. Bergholtz, "Non-hermitian extensions of higher-order topological phases and their biorthogonal bulk-boundary correspondence," Phys. Rev. B **99**, 081302 (2019).
[47] Zhiwang Zhang, María Rosendo López, Ying Cheng, Xiaojun Liu, and Johan Christensen, "Non-hermitian sonic second-order topological insulator," Phys. Rev. Lett. **122**, 195501 (2019).
[48] Ching Hua Lee, Linhu Li, and Jiangbin Gong, "Hybrid higher-order skin-topological modes in nonreciprocal systems," Phys. Rev. Lett. **123**, 016805 (2019).
[49] Mao Lin and Taylor L. Hughes, "Topological quadrupolar semimetals," Phys. Rev. B **98**, 241103 (2018).
[50] $\mathcal{M}_x = \sigma^1\kappa^3$, $\mathcal{M}_y = \sigma^1\kappa^1$, $\mathcal{M}_z = I$, inversion symmetry $\mathcal{I} = \sigma^0\kappa^2$, and spinless time-reversal $\mathcal{T} = K$ ().
[51] Supplementary material.
[52] Kazuki Sone, Yuto Ashida, and Takahiro Sagawa, "Exceptional non-hermitian topological edge mode and its application to active matter," Nature communications **11**, 1–11 (2020).
[53] Alex Y. Song, Xiao-Qi Sun, Avik Dutt, Momchil Minkov, Casey Wojcik, Haiwen Wang, Ian A. D. Williamson, Meir Orenstein, and Shanhui Fan, "$\mathcal{PT}$-symmetric topological edge-gain effect," Phys. Rev. Lett. **125**, 033603 (2020).
[54] The topological invariant for the exceptional ring is defined by the Hamiltonian $H(k_y, k_z)$ with the open boundary condition in the x-direction [29]. Because of chiral symmetry Γ_0, $i\Gamma_0 \otimes H(k_y, k_z)$ is Hermitian, and it has a (conventional) gap at zero energy except on the exceptional ring. Therefore, we can count the number of negative energy states of $i\Gamma_0 \otimes H(k_y, k_z)$ except on the exceptional ring. The number of negative energy states can be different between the inside and the outside of the exceptional ring, and the difference gives the topological invariant for the exceptional ring. ().
[55] Li Ge and Hakan E. Türeci, "Antisymmetric $\mathcal{PT}$-photonic structures with balanced positive- and negative-index materials," Phys. Rev. A **88**, 053810 (2013).
[56] Note that due to explicit k_z dependence, the non-Hermitian term vanishes at high-symmetry points of k_z.

Therefore, a avoided region appear in the spectrum and forms two patches of ESs on opposite momenta in the vicinity of $k_z = 0, \pi$ of bulk spectrum. ().

[57] William A. Wheeler, Lucas K. Wagner, and Taylor L. Hughes, "Many-body electric multipole operators in extended systems," Phys. Rev. B **100**, 245135 (2019).

[58] Byungmin Kang, Ken Shiozaki, and Gil Young Cho, "Many-body order parameters for multipoles in solids," Phys. Rev. B **100**, 245134 (2019).

[59] Seishiro Ono, Luka Trifunovic, and Haruki Watanabe, "Difficulties in operator-based formulation of the bulk quadrupole moment," Phys. Rev. B **100**, 245133 (2019).

[60] Kohei Kawabata, Masatoshi Sato, and Ken Shiozaki, "Higher-order non-hermitian skin effect," Phys. Rev. B **102**, 205118 (2020).

[61] Ryo Okugawa, Ryo Takahashi, and Kazuki Yokomizo, "Second-order topological non-hermitian skin effects," Phys. Rev. B **102**, 241202 (2020).

[62] Yongxu Fu, Jihan Hu, and Shaolong Wan, "Non-hermitian second-order skin and topological modes," Phys. Rev. B **103**, 045420 (2021).

[63] Liang Feng, Ramy El-Ganainy, and Li Ge, "Non-hermitian photonics based on parity–time symmetry," Nature Photonics **11**, 752–762 (2017).

[64] Peng Peng, Wanxia Cao, Ce Shen, Weizhi Qu, Jianming Wen, Liang Jiang, and Yanhong Xiao, "Anti-parity–time symmetry with flying atoms," Nature Physics **12**, 1139–1145 (2016).

[65] Jin-Hui Wu, M. Artoni, and G. C. La Rocca, "Non-hermitian degeneracies and unidirectional reflectionless atomic lattices," Phys. Rev. Lett. **113**, 123004 (2014).

[66] Diana A Antonosyan, Alexander S Solntsev, and Andrey A Sukhorukov, "Parity-time anti-symmetric parametric amplifier," Optics letters **40**, 4575–4578 (2015).

[67] Qiang Wei, Xuewei Zhang, Weiyin Deng, Jiuyang Lu, Xueqin Huang, Mou Yan, Gang Chen, Zhengyou Liu, and Suotang Jia, "Higher-order topological semimetal in acoustic crystals," Nature Materials , 1–6 (2021).

[68] Li Luo, Hai-Xiao Wang, Zhi-Kang Lin, Bin Jiang, Ying Wu, Feng Li, and Jian-Hua Jiang, "Observation of a phononic higher-order weyl semimetal," Nature Materials **20**, 794–799 (2021).

[69] Xiang Ni and Andrea Alù, "Higher-order topolectrical semimetal realized via synthetic gauge fields," APL Photonics **6**, 050802 (2021).

[70] Huahui Qiu, Meng Xiao, Fan Zhang, and Chunyin Qiu, "Higher-order dirac sonic crystals," (2020), arXiv:2012.00251 [cond-mat.other].